

PHYSICAL REVIEW B

CONDENSED MATTER AND MATERIALS PHYSICS

THIRD SERIES, VOLUME 62, NUMBER 4

15 JULY 2000-II

RAPID COMMUNICATIONS

Rapid Communications are intended for the accelerated publication of important new results and are therefore given priority treatment both in the editorial office and in production. A Rapid Communication in Physical Review B may be no longer than four printed pages and must be accompanied by an abstract. Page proofs are sent to authors.

Enhancement and suppression of thermal emission by a three-dimensional photonic crystal

Shawn-Yu Lin, J. G. Fleming, E. Chow, and Jim Bur

Sandia National Laboratories, P.O. Box 5800, Albuquerque, New Mexico 87185

K. K. Choi and A. Goldberg

US Army Research Laboratories, 2800 Powder Mill Road, Adelphi, Maryland 20783

(Received 20 January 2000; revised manuscript received 19 April 2000)

The emission and detection of electromagnetic radiation are essential optical processes that govern performance of lasers, detectors and solar cells. Through light-photonic crystal interaction, a three-dimensional (3D) photonic crystal offers a way to alter such optical processes. Experimental realization is done by building a thin slab of 3D photonic crystal onto a silicon material. The 3D crystal structure is found to be highly effective in suppressing silicon thermal radiation in the photonic band gap spectral regime. Emission is also enhanced in the photonic passbands. At passband resonant frequencies, a thin slab of 3D photonic crystal actually acts like a planar blackbody.

A three-dimensional (3D) photonic crystal is an artificially engineered, periodic dielectric material that exhibits bands and gaps in its photonic density-of-states (DOS) spectrum.¹⁻⁵ Inside a photonic band gap, photonic DOS vanishes, and no electromagnetic (EM) waves are allowed to propagate. Within the photonic pass bands, oscillations in DOS occur, corresponding to transmission resonances inside the photonic crystal.⁶

One unique application of the 3D photonic band gap is the modification of spontaneous emission.⁷ The band gap is used to establish a strongly confined optical environment, called cavity, for light trapping and size quantization. The quantization alters photonic DOS inside the cavity, leading to the modification of spontaneous emission of atoms or semiconducting materials. Experimental demonstration of such a modification has been reported using the so-called OPAL based 3D photonic crystal.⁸ The same photonic band gap effect may also be used to suppress thermal emission, as it is also an EM radiation. In this case, the band gap does not alter the DOS of the thermal radiating elements, but only acts as a radiation filter. On the other hand, despite the intricate DOS spectrum, the consequences of the 3D photonic passband are largely unknown, either theoretically or experimentally. Its potential influence on the emission or absorption process of a material is also unexplored.

Recently, results of a theoretical calculation for a 1D photonic crystal suggest the existence of antireflection nodes in the allowed band.⁹ Such nodes are shown to originate from 1D transmission resonance. Similarly, in the allowed band of a 3D photonic crystal, antireflection nodes should also exist. At such node frequencies, a complete absorption of thermal radiation incident from all 3D angles is expected.

In the work reported here, a silicon 3D photonic crystal is created and its effect on silicon thermal emission studied. The 3D crystal is found to be highly effective in suppressing silicon thermal radiation in the photonic band gap spectral regime. In the photonic passbands, thermal emission intensity is enhanced. At transmission resonance frequencies, it even reaches the blackbody limit. The ability of 3D photonic crystals to alter surface emittance and absorptance may enhance performance of lasers, detectors,¹⁰ solar cells, and infrared thermal image control.¹¹

The 3D photonic crystal has a diamond crystal symmetry¹² and was fabricated using an advanced silicon processing. Details of the fabrication process have been reported previously.¹³ Briefly, the crystal consists of layers of one-dimensional silicon rods with a stacking sequence that repeats itself every four layers, repeating distance c . Within each layer, the axes of the rods are parallel to each other with

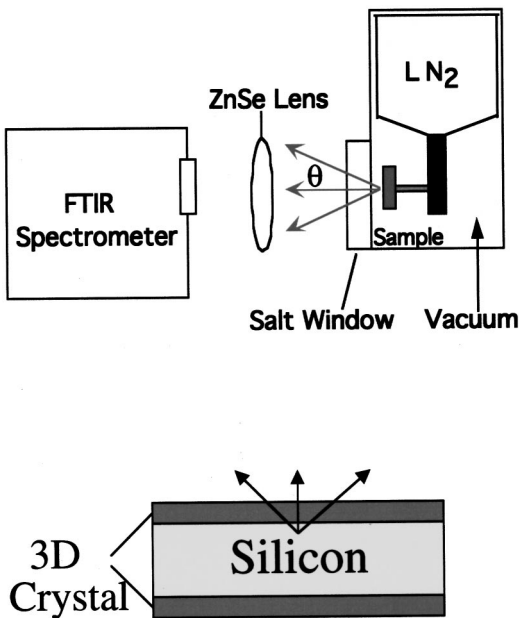


FIG. 1. (a) Schematic diagram of the thermal emission measurement setup. The sample is placed in a vacuum chamber, supported by a 2-in.-long ceramic post that connects to a liquid-nitrogen-cooled cold stage and heated to $T \sim 410$ K during measurement. (b) Schematic diagram of a photonic-crystal test sample. Two pieces of identical 3D silicon photonic crystals were bound back-to-back. The silicon thermal emission is emitted through the 3D crystal top surface.

a pitch of $d = 4.2 \mu\text{m}$. The orientation of the axes is rotated by 90° between adjacent layers. Between every other layer, the rods are shifted relative to each other by $0.5d$.¹² The resulting structure has a face-center-tetragonal lattice symmetry. For the special case of $c/d = 1.414$, the lattice can be derived from a face-centered-cubic unit cell with a basis of two rods, i.e., the diamond lattice. The width of the rod is $W = 1.2 \mu\text{m}$, and the filling fraction of the high dielectric silicon material is 28%. At this filling fraction, the 3D crystal has a large photonic band gap covering the infrared wavelength range from $\lambda = 9\text{--}15 \mu\text{m}$.¹³

To measure infrared thermal emission, the experimental setup must be properly configured such that background thermal emission is eliminated and, at the same time, sample emission intensity enhanced. To achieve this goal, the sample was placed in a liquid-nitrogen cooled ($T = 77$ K) vacuum chamber and heated to $T \sim 410$ K. In Fig. 1(a), a schematic of such a measurement setup is shown. At low temperatures, $T = 77$ K, the unwanted thermal emission from the sample holder is minimized. In vacuum conditions, no air is heated and this contributes to background thermal emission. Heating is also necessary to increase the thermal emission intensity. To insulate the heated sample from the liquid-nitrogen cold bath, the sample was mounted to a 2-in.-long ceramic post. The thermal radiation first passes through a salt window, is collected by a ZnSe lens, and finally is fed into a Fourier transform infrared spectrometer for spectral analysis. A DTGS infrared photodetector was used for infrared signal detection. The salt window is transparent up to $\lambda \sim 12 \mu\text{m}$, is 50% transparent at $\lambda \sim 17 \mu\text{m}$, and has a long wavelength cutoff at $\lambda \sim 21 \mu\text{m}$. The photodetector has a fairly flat spectral response in the infrared.

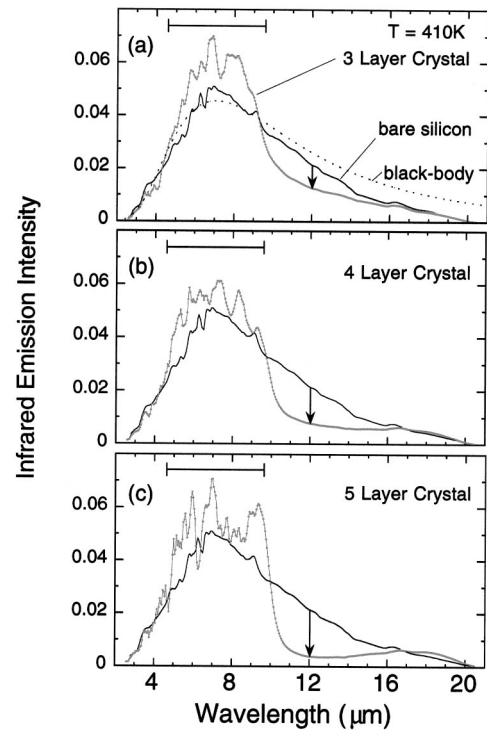


FIG. 2. The measured thermal emission spectra taken from a silicon sample (solid line) and 3D photonic crystal samples (red solid dots) of different numbers of layers, $n = 3, 4$, and 5 , respectively. Also plotted (the dashed line) is a theoretical blackbody radiation curve for a temperature of 410 K. For the 3D crystal sample, emission intensity in the $\lambda = 10\text{--}16 \mu\text{m}$ range is greatly suppressed, indicative of a 3D photonic band gap. The emission intensity at a $\lambda \sim 5\text{--}9 \mu\text{m}$ range for all three crystal samples exceeds that of the silicon.

The detail of the sample arrangement and experimental configuration is shown in Fig. 1(b). The sample consists of two pieces of identical 3D silicon photonic crystal bound back-to-back, having the silicon layer sandwiched on both sides by a thin slab of 3D crystal. The spacing between the two layers of photonic crystal is about 1.2 mm. The boundary defined by silicon and the 3D photonic crystal slab is planar. This is in contrast to a microcavity structure, in which the boundary is a closed contour,^{14,15} commonly used to study light-photonic crystal interaction.

In Fig. 2(a), the emission spectrum taken from a three-layer photonic crystal sample and a bare silicon sample are shown as red solid dots and a line, respectively. At both the long ($>18 \mu\text{m}$) and short ($<4 \mu\text{m}$) wavelength limits, the two curves agree well with each other. On the other hand, at the midwavelength range ($\lambda = 10$ to $16 \mu\text{m}$), emission from the crystal sample is clearly suppressed. The strongest suppression is at $\lambda \sim 12 \mu\text{m}$ and is indicated by the down arrow. The suppression of thermal emission becomes stronger as the number of 3D crystal layers is increased from $n = 3, 4$ to 5 [see Figs. 2(b) and 2(c)]. The suppression is indicative of the absence of photonic DOS in the band gap regime that forbids the emission of infrared radiation in all 4π angles.

It is noted that the emission intensity at $\lambda \sim 5\text{--}9 \mu\text{m}$ range for the three-layer crystal sample exceeds that of silicon emission by about 30%. The enhancement is also clearly evident for the four- and five-layer samples. For the five-

layer sample, the contrast between emission suppression and enhancement is quite dramatic. Specifically, following the strong suppression in the gap regime, the emission intensity quickly rises on both sides of the band gap, intercepts the bare-Si reference curve at $\lambda=10$ and $17 \mu\text{m}$, and finally exceeds silicon emission. Pronounced oscillations also appeared in the spectrum, but only at the shorter $\lambda=5-9 \mu\text{m}$ wavelength side. Also, the oscillation pattern reveals more detailed features as the number of layers is increased. The observed oscillations and their dependence on the number of crystal layers suggest a correlation to the oscillating photonic DOS in a 3D photonic crystal.

For comparison purposes, a blackbody radiation curve calculated for a temperature of 410 K is also shown in Fig. 2(a) as a dashed line. The silicon emission curve and blackbody curve agree well with each other, except for the gradual deviation at $\lambda>12 \mu\text{m}$. This agreement is consistent with the fact that silicon is a graybody and independently confirms the measured temperature. The line shape of a graybody is identical to that of a blackbody, but its emission intensity is weaker. The deviation is not intrinsic to the silicon emission and is caused by the long wavelength cutoff of the optical window material, as mentioned earlier.

To obtain the absolute suppression and enhancement efficiency of a 3D photonic crystal, the two measured spectra, $f_0(\lambda)$ and $f(\lambda)$, must be normalized. The spectrum $f_0(\lambda)$ serves as a reference and is directly related to the intrinsic silicon emissivity, $E_{(\lambda)}$ by $f_0 \cong E_0(\lambda)W(\lambda)D(\lambda)$. Here $W(\lambda)$ represents propagation loss, such as water absorption, as thermal emission passes through the spectrometer and reaches the photodetector. $D(\lambda)$ represents the combined optical window and photodetector responses. Similarly, the spectrum, $f(\lambda)$, is related to the modified emissivity, $E(\lambda)$ by $f \cong E(\lambda)W(\lambda)D(\lambda)$. By dividing $f(\lambda)$ into $f_0(\lambda)$, the window/detector response and water absorption loss are normalized, and a normalized emission efficiency, $E(\lambda)/E_0(\lambda)$, is obtained. Because of water absorption and background thermal radiation, the normalized emission efficiency has an experimental error of about $\pm 10\%$.

In Fig. 3(a), the normalized emission efficiency is plotted as a function of wavelength for the five-layer crystal sample. A clear and strong dip is observed at $\lambda \sim 12 \mu\text{m}$ along with a broad bandwidth of $\Delta\lambda \sim 6 \mu\text{m}$. The dip minimum of $\sim 15\%$ is slightly higher than that observed, $\sim 8\%$, in a straight transmission measurement with light propagating along $\langle 001 \rangle$ direction [Fig. 3(b)]. In the gap regime, thermal spectrum measures tunneling emission over all angles, which is slightly higher than that measured solely along $\langle 001 \rangle$, and causes the difference. Indeed, thermal emission is three-dimensional in nature and the measured gap is truly a 3D photonic band gap. This result is consistent with the presence of a photonic band gap in our 3D photonic crystal structure.

In the inset of Fig. 3(a), the suppression efficiency vs the number of layers of photonic crystal is shown as a semilog plot at $\lambda=12, 14, 15,$ and $16 \mu\text{m}$, respectively. The straight lines show that the suppression depends exponentially on n and is consistent with the tunneling nature of light in the band gap regime. The straight line also predicts that a suppression of 99% (or equivalently a 1% emissivity) may be achieved at $\lambda=12 \mu\text{m}$ using an eight-layer photonic crystal. This value is to be compared to an emissivity value of 0.50

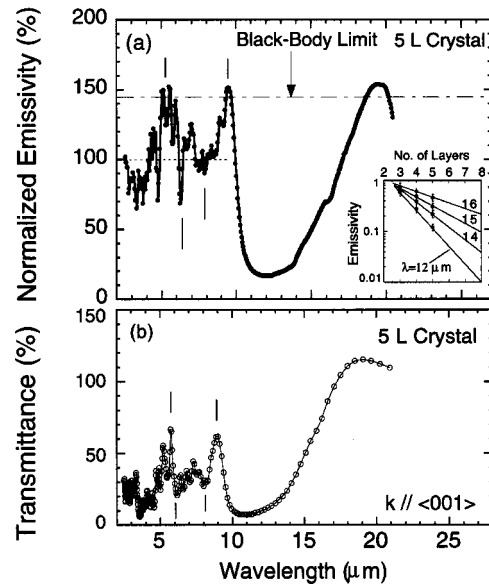


FIG. 3. (a) Normalized emission efficiency vs wavelength for a five-layer photonic crystal sample. A clear and strong dip is observed at $\lambda \sim 12 \mu\text{m}$ along with a broad bandwidth of $\Delta\lambda \sim 6 \mu\text{m}$. At the pass band wavelengths, $\lambda \sim 5-10 \mu\text{m}$ and $\lambda \sim 17-20 \mu\text{m}$, an unusually high emission intensity is observed. At the oscillation peaks, the intensity reaches the blackbody limit (the dashed line) within $\pm 5\%$. In the inset, normalized efficiency is plotted in a semi-log scale as a function of the number of layers of 3D crystal. Thermal emission suppression of 99% (or equivalently a 1% emissivity) may be achieved at $\lambda=12 \mu\text{m}$ using an eight-layer 3D photonic crystal. (b) Transmission spectrum taken from the same five-layer photonic crystal sample. The passband oscillations correlate well with the oscillations in the emittance spectrum.

for commonly used aluminum paint and 0.15 for copper.¹⁶ Even for the silvered mirror, one of the lowest emissivity materials, emissivity is 0.02.¹⁶ Furthermore, a 3D silicon photonic crystal is more robust against oxidation for temperatures up to 800 to 900 $^{\circ}\text{C}$ and is ideal for achieving an ultralow and controllable thermal emission.

Another interesting feature of the data is the unusually high emission at the passband wavelengths, $\lambda \sim 5-10 \mu\text{m}$ and $\lambda \sim 17-20 \mu\text{m}$. This value not only exceeds the 30 to 70% straight transmission amplitude [Fig. 3(b)], but also exceeds the silicon emission value, 100%. At oscillation maxima, the emission reaches the blackbody limit (the dashed line) within $\pm 5\%$.¹⁷ In other words, the 3D crystal layer transforms a silicon material from a “graybody” into a “blackbody” at the oscillation peaks. The 3D crystal/Si structure may then be thought of as a composite material with total transparency. This property may find important solar-cell applications because it is capable of enhancing solar energy absorption efficiency by a large 30 to 50%.

Analogous to the prediction made for a 1D photonic crystal,⁹ the observed emission enhancement for our 3D crystal may also be attributed to photonic transmission resonances. Due to multiple coherent scattering of light inside a photonic crystal, resonance occurs at certain frequencies and total transmission of light becomes possible. In a photonic crystal, transmission resonances manifest themselves as maxima (or peaks) in the photonic DOS spectrum. In Fig. 3(b), the peaks and dips in passband transmittance are caused

by such resonances in the photonic DOS. Comparing the emittance and transmittance spectra, shown in Figs. 3(a) and 3(b), a clear resemblance of passband oscillations is observed. In particular, the peaks at $\lambda \sim 5.2$ and $9.4 \mu\text{m}$, indicated by vertical bars, in the emittance data correlate with the transmission peaks at $\lambda \sim 5.5$ and $9.0 \mu\text{m}$. The dip at $\lambda \sim 7 \mu\text{m}$ also shows up in both spectra. The thermal emission is 3D in nature and measured an average DOS over a range of angle ($\theta \sim 40^\circ$) defined by the collecting lens. This angle covers a significant portion, but not all, of the first Brillouin zone of our 3D structure, i.e., ranges from Γ - X' to Γ - K , and to halfway between Γ - K and Γ - L symmetry points.¹³ This weighted averaging causes the slight shift from $\lambda \sim 9.0$ to $9.4 \mu\text{m}$. The respective peak positions at $\lambda \sim 20 \mu\text{m}$ also agree well with each other. This close correlation suggests that the emission enhancement is indeed a DOS effect. This work

presents thermal emission enhancement brought about by a 3D photonic crystal effect.

In summary, the observation of thermal emissivity modification from silicon is reported using a 3D photonic crystal. The 3D crystal is found to be highly effective in suppressing the thermal emission. The discovery of emission enhancement leads us to conclude that a thin slab of 3D crystal actually acts like a blackbody at transmission resonances. Furthermore, through photonic DOS engineering, a 3D photonic crystal offers a fundamentally different way for altering surface emissivity and absorption.

The authors also thank Dr. S. R. Kurtz for technical assistance. This work was supported by the United States Department of Energy under Contract DE-AC04-94AL85000. Sandia is a multiprogram laboratory operated by Sandia Corporation, a Lockheed Martin Company, for the United States Department of Energy.

-
- ¹E. Yablonovitch *et al.*, Phys. Rev. Lett. **67**, 2295 (1991); S. John *ibid.* **58**, 2486 (1987); J. D. Joannopoulos, R. D. Meade, and J. N. Winn, *Photonic Crystals* (Princeton, New York, 1995).
- ²K. M. Leung and Y. F. Lu, Phys. Rev. Lett. **65**, 2646 (1990).
- ³Z. Zhang and S. Satpathy, Phys. Rev. Lett. **65**, 2650 (1990).
- ⁴K. M. Ho *et al.*, Phys. Rev. Lett. **65**, 3152 (1990).
- ⁵W. M. Robertson *et al.*, Phys. Rev. Lett. **68**, 2023 (1992).
- ⁶J. M. Bendickson *et al.*, Phys. Rev. E **53**, 4107 (1996).
- ⁷E. Yablonovitch, Phys. Rev. Lett. **58**, 2059 (1987).
- ⁸E. P. Petrov *et al.*, Phys. Rev. Lett. **81**, 77 (1998); S. G. Romanov *et al.*, Appl. Phys. Lett. **75**, 1057 (1999); T. Yamasaki *et al.*, *ibid.* **72**, 1957 (1998); K. Yoshino *et al.*, *ibid.* **73**, 3506 (1998).
- ⁹C. M. Cornelius and J. Dowling, Phys. Rev. A **59**, 4736 (1999).
- ¹⁰See, for example, B. E. A. Saleh and M. C. Teich, *Fundamentals of Photonics* (John Wiley & Sons, New York, 1991), Chap. 17, pp. 648–649.
- ¹¹F. K. Hopkins, Opt. Photonics News **9**, 32 (1998); A. P. Owen *ibid.* **9**, 34 (1998).
- ¹²K. M. Ho *et al.*, Solid State Commun. **89**, 413 (1994).
- ¹³S. Y. Lin *et al.*, Nature (London) **394**, 251 (1998).
- ¹⁴E. Yablonovitch *et al.*, Phys. Rev. Lett. **67**, 3380 (1991).
- ¹⁵S. Y. Lin *et al.*, Phys. Rev. B **59**, R15 579 (1999).
- ¹⁶E. L. Dereniak and G. D. Boreman, *Infrared Detectors and Systems* (John Wiley & Sons, New York, 1996), Chap. 2, pp. 72–76. For a general reference to infrared emission and detection.
- ¹⁷In the absence of photonic crystal layers, the reflectivity of silicon is given by $R = [(n-1)/(n+1)]^2 = 0.31$ and its absorptance is 0.69. Here, n is the silicon refractive index and its value is 3.6. The blackbody absorptance is 1.00 and is 45% higher than the silicon absorptance.